Research paper

Linking stem growth respiration to the seasonal course of stem growth and GPP of Scots pine

Tommy Chan[1,2,3], Frank Berninger[1], Pasi Kolari[2], Eero Nikinmaa[1] and Teemu Hölttä[1]

[1]Institute for Atmospheric and Earth System Research/Forest Sciences, Faculty of Agriculture and Forestry, University of Helsinki, PO Box 27, 00014 Helsinki, Finland; [2]Institute for Atmospheric and Earth System Research/Physics, Faculty of Science, University of Helsinki, PO Box 68, 00014 Helsinki, Finland; [3]Corresponding author (tommy.chan@helsinki.fi)

Current methods to study relations between stem respiration and stem growth have been hampered by problems in quantifying stem growth from dendrometer measurements, particularly on a daily time scale. This is mainly due to the water-related influences within these measurements that mask growth. A previously published model was used to remove water-related influences from measured radial stem variations to reveal a daily radial growth signal ($\hat{\Delta} G_m$). We analysed the intra- and inter-annual relations between $\hat{\Delta} G_m$ and estimated growth respiration rates (R_g) on a daily scale for 5 years. Results showed that R_g was weakly correlated to stem growth prior to tracheid formation, but was significant during the early summer. In the late summer, the correlation decreased slightly relative to the early summer. A 1-day time lag was found of $\hat{\Delta} G_m$ preceding R_g. Using wavelet analysis and measurements from eddy covariance, it was found that R_g followed gross primary production and temperature with a 2 and 3 h time lag, respectively. This study shows that further in-depth analysis of in-situ growth and growth respiration dynamics is greatly needed, with a focus on cellular respiration at specific developmental stages, its woody tissue costs and linkages to source–sink processes and environmental drivers.

Keywords: dendrometers, eddy covariance, GPP, growth, growth efficiency, radial variations, respiration.

Introduction

Stem growth, net primary production (NPP) and the physiological costs to maintain and grow woody tissue have been of great interest because of their contribution to forest carbon budgets. In particular, the components of NPP, gross primary production (GPP) and autotrophic respiration have been studied extensively in relation to biomass growth and carbon budgets (Ryan et al. 1997, Xiao et al. 2003, Goulden et al. 2011). In relation to stand or ecosystem energy budgets, autotrophic respiration, for example, can consume anywhere from 30% to 70% of the total carbon fixed for maintenance and tissue construction (Sprugel and Benecke 1991, Ryan et al. 1997). Usually, respiration is studied at the ecosystem level with the eddy covariance technique, which can estimate both GPP and ecosystem respiration (which includes autotrophic and heterotrophic components) (Desai et al. 2008).

Yet the contribution of different tree organs to ecosystem respiration and individual trees is unclear, particularly as methodologies for measuring stem respiration and stem growth differ. This ultimately produces substantially varying results.

A common method for measuring stem respiration is with an open flow-through chamber installed onto a stem segment. By calculating the difference between the carbon dioxide (CO_2) concentration entering and exiting the chamber, the stem CO_2 efflux (E_S) can be determined. Since E_S from a stem segment is the measured gas exchange between woody stem and external atmosphere, it is often associated with the rate of physiologically active respiration of the living tissues (i.e., phloem, cambium and xylem parenchyma) (Saveyn et al. 2008). However, the relationship between E_S and actual respiration is difficult to assess, as

CO_2 is carried to and from the point of measurement vertically along the xylem (Teskey and McGuire 2002, Teskey et al. 2008, Hölttä and Kolari 2009, Bloemen et al. 2013).

One approach to quantifying respiration, with respect to stem carbon budgeting, is by separating E_S into two functional components: respiration costs used to build new dry matter (growth respiration) and respiration needed to maintain the life processes of living cells (maintenance respiration) (Amthor 2012). By estimating either the growth or maintenance respiration component first, the difference between total respiration and the estimate will reveal the other component. Various studies have estimated the growth component first, revealing the maintenance component as the difference (Ryan et al. 1994, Carey et al. 1996), but estimating the maintenance component first remains the most widely preferred method (Stockfors and Linder 1998, Maier 2001). One method to separate total stem CO_2 efflux into maintenance respiration and growth respiration components is the mature tissue method (Amthor 2012). This method assumes that the total respiration from mature tissue (i.e., tissue that is no longer growing) may be attributed to the maintenance respiration component. Thus, calculating maintenance respiration rates outside of the growing season (typically before day of year (DOY) 130 and after DOY 240) can be used to estimate annual maintenance respiration rates.

Separating E_S into these components allows for further investigation of stem carbon budgeting and tissue costs. However, this separation requires caution—estimation of maintenance and growth respiration rates may not be wholly independent of one another (Lavigne et al. 1996). Therefore, it can be difficult to correctly separate the two components. In addition, the growth respiration derived from the mature tissue method has a tendency to be estimated higher compared with other theoretical methods (Sprugel and Benecke 1991), suggesting that the products of growth respiration are more demanding—and possibly that all woody respiration during the growing season is solely related to growth regardless of is partitioning.

It has been reported that both external and internal drivers regulate E_S (Maier et al. 2010). For example, studies have extensively documented influences from water (Rodríguez-Calcerrada et al. 2014, Salomón et al. 2016), temperature (Stockfors and Linder 1998, Zha et al. 2004, Gruber et al. 2009, Brito et al. 2010, Reich et al. 2016), sap flow (Negisti 1972, Negisi 1975, Bowman et al. 2005, Gansert and Burgdorf 2005), carbohydrate supply (Maunoury-Danger et al. 2010) and the phenological phases of the tree (Asshoff et al. 2006). In principle, the growth respiration component of E_S is correlated with stem growth with a short time lag (Ryan 1990). However, previous studies have reported inconsistent results. For example, studies correlating stem growth rate (SGR) and stem growth respiration rates (R_g) showed a lag range varying from 0 to 40 days (Zumer 1969, Edwards and Hanson 1996, Zha et al. 2004). One factor that may contribute to these large differences is the measurement

technique. Stem growth and R_g correlation studies mainly utilize dendrometers to measure stem radius/diameter increment—a proxy for volumetric stem growth. However, it is clear that growth taken directly from these instruments also includes water-related changes (Daudet et al. 2005, Mencuccini et al. 2013, Chan et al. 2016, Zweifel 2016). These changes (although reversible and small on a seasonal scale) are typically larger than growth on a daily scale, and can therefore mask quantifiable short-term (e.g., daily) growth. Studies have circumvented this problem by using dendrometer measurements on a bi-weekly (Maier 2001), monthly (Vose and Ryan 2002, Zha et al. 2004) and annual (Araki et al. 2015) scale. However, the consequence is the loss of daily dynamics and the possibility to link R_g directly to SGR or environmental conditions. It is, therefore, important to analyse growth on a daily scale in order to understand respiration dynamics throughout the year, especially during the growing season.

It has been suggested that R_g is proportional to SGR, while temperature should not affect it apart from influencing the SGR (Lavigne and Ryan 1997, Loveys et al. 2002, Vose and Ryan 2002). Additionally, changes in chemical composition of the wood can affect R_g by increasing or decreasing construction cost. As woody tissue progresses through different stages of physiological or biochemical changes during the growing season, it is possible to explain whether R_g varies in relation to these different stages (Vose and Ryan 2002). This has been supported in a study at the ecosystem level, where the intra-annual changes of GPP and E_S were highly correlated (Zha et al. 2004). Stem growth undergoes three predominant processes before maturation: cell division, cell enlargement and cell wall thickening/deposition (Rossi et al. 2006a). Growth derived from dendrometers show only the influence of cell division and enlargement processes to tissue dimension, whereas growth derived from microcores can identify all three processes (Rossi et al. 2006a, Deslauriers et al. 2007, Mäkinen et al. 2008). On the other hand, carbon-fixation observed from eddy covariance measurements refers to the difference between ecosystem photosynthesis and respiration over a given time period in a given area, and thus cannot be used to observe cellular growth (Pretzsch 2009). However, as GPP also provides resources for both growth and respiration analysis, comparison with tree-level growth respiration dynamics may also prove valuable. By separating growth into distinct phases, each representing the predominant growth process, intra-annual R_g to growth dynamics can be studied. This has been shown in previous studies, but only on specific days (Stockfors and Linder 1998) and on a monthly scale (Vose and Ryan 2002). When exactly these correlations appear and what metabolic processes occur during these times have yet to be further explored.

In this study, we investigate the relationship and dynamics between GPP, growth and growth respiration on a daily time scale to provide a physiological understanding of tree growth. We link this relationship to whole year and apparent (i.e., intra-annual)

growth efficiency by observing the year's biomass growth. We also relate derived estimates of GPP from eddy covariance measurements to the study. The SGR was estimated using a previously published model (Chan et al. 2016) on field-measured dendrometer data of *Pinus sylvestris* L. (Scots pine). We hypothesize that the dynamics between growth, growth respiration and GPP can be observed during the whole year if we apply the model to separate the growth component from dendrometer measurements. Our objectives were: (i) to compare the dynamics of R_g with SGR derived from the corrected water-related model estimate and direct (i.e., raw) radial stem measurements at different growth phases; (ii) to identify the time lag between R_g and SGR; (iii) to calculate the annual budget for woody-tissue respiration; and (iv) compare the dynamics of R_g to both GPP and temperature using wavelet analysis.

Materials and methods

Site description

The study site is located at SMEAR II (System for Measuring Forest Ecosystem-Atmosphere Relationships II) research station in Hyytiälä, Finland (61°51′N, 24°17′E, 170 m above sea level). The study site is an even-aged, 51-year-old Scots pine forest, belonging to the southern boreal zone. The forest area is of medium site quality (Vaccinium-type) according to the Cajander class system (Cajander 1909) (see Vesala et al. (2005) for detailed description). The mean height of the stand is 17.4 m with a mean diameter at breast height (1.3 m) of 18 cm, with a typical stemwood growth rate of $8\ m^3\ ha^{-1}\ year^{-1}$ (2014 data). The yearly average GPP, TER (total ecosystem respiration) and NEE (net ecosystem CO_2 exchange) during the growing period (April–October; 1997–2014) from eddy covariance measurements over the stand is 5.34, 3.41 and $1.92\ \mu mol\ m^{-2}\ s^{-1}$, respectively (refer to Table 1 for the main terminology used). The parent material of the soil is composed of sandy and coarse silty glacial till and the soil is a Haplic Podzol. The mean annual precipitation of the area is 713 mm, with a mean annual air temperature of 3.3 °C. The warmest and coldest months are July (mean +15.3 °C) and January (mean −8.9 °C), respectively. The growing season generally begins in late April and ends around early September.

Environmental variables and stand level fluxes

Year-round field data of air temperature (°C) was recorded continuously from a tower at a height of 8.4 m at 1-min intervals and measured with radiation-shielded pt-100-type resistance thermometer sensors. The estimate of GPP was derived from eddy covariance measurements of NEE. Gross primary production ($\mu mol\ m^{-2}\ s^{-1}$) was calculated by subtracting a temperature-driven model of TER from the measured NEE (see Kolari et al. (2009) for further details). The model was based on a periodic temperature response from night-time measurements. In total, five trees were used in the study (see Table 2): three trees were

Table 1. A summary of the terminology and definitions used.

Terminology	Definition
E_s	Measured stem CO_2 efflux ($\mu g\ CO_2\ m^{-2}\ s^{-1}$)
R_g	Growth respiration rate ($\mu g\ CO_2\ m^{-2}\ s^{-1}$)
R_m	Maintenance respiration rate ($\mu g\ CO_2\ m^{-2}\ s^{-1}$)
SGR	Stem growth rate
GPP	Gross primary production ($\mu mol\ m^{-2}\ s^{-1}$)
$\hat{\Delta}G_m$	Modelled growth; model-estimated accumulated growth during a season—i.e., estimated cambial growth and change of radius due to osmotic concentration variation (mm)
$\Delta\hat{\Delta}G_m$	Modelled daily growth rate; daily derivative of $\hat{\Delta}G_m$, representing the daily estimated growth rate (mm day^{-1})
D_w	Raw growth; measured whole-stem radial variation (mm)
ΔD_w	Raw daily growth rate; daily derivative of D_w, represented by the daily growth rate (mm day^{-1})
D_b	Measured inner-bark radial variation (mm)
D_x	Measured xylem radial variation (mm)
Q_{10}	Temperature coefficient of respiration
Y	Growth efficiency
CWT	Continuous wavelet transform
WC	Wavelet coherence

Table 2. The number of trees monitored in the study for each year, and the type of measurements performed on each tree. Statistical analysis was performed on trees 1, 4 and 5. Trees 2 and 3 were used to corroborate the growth model. In the current study, trees 4 and 5 are denoted as 2015a and 2105b, respectively.

Year	Tree no.	Measurements
2007–09, 2011	1	Radial stem variations, stem CO_2 efflux
	2	Radial stem variations
	3	Radial stem variations
2015	4	Radial stem variations, stem CO_2 efflux
	5	Radial stem variations, stem CO_2 efflux

measured continuously from 2007 to 2009 and in 2011, and two trees in 2015. Of the trees monitored from 2007 to 2009 and in 2011, in one tree both radial stem variations and stem CO_2 efflux were measured, while in the remaining two only radial stem variations were measured. To distinguish the trees measured in 2015, one tree was denoted as 2015a and the other as 2015b. In consideration of the fact that the stem CO_2 efflux chamber was installed on one tree for this study from 2007 to 2011, further data analysis was performed from that tree only, and dendrometer measurements from the other trees were used to validate modelled growth (see Figure S1 available as Supplementary Data at *Tree Physiology* Online).

Dendrometer measurements

Radial stem variations, expressed in mm, were measured using two LVDT dendrometers (linear variable-displacement transducers; model AX/5.0/S, Solartron Inc., West Sussex, UK) at a height of ~15 m, below the canopy. Dendrometers were installed on three trees for years 2007–09 and 2011, and on two trees for

year 2015. The dendrometers were connected to a data logger (21×, Campbell Scientific Ltd, Leics, UK) by means of multiplexers (SDMX50, Campbell Scientific Ltd) and measured continuously at 1-min intervals. The dendrometers were secured to a rectangular stainless-steel frame (Sandvik 1802 Steel, Sandvik, Sandvixen, Sweden) and spaced 30 mm apart. The frame was then affixed onto the tree with screws using attachment plates (Sevanto et al. 2005). One dendrometer measured xylem radial variation (D_x). The head of this dendrometer rested against a small screw that was inserted ~10 mm through the outer- and inner-bark, into the superficial part of the existing xylem. The second dendrometer measured whole-stem radial variation (D_w), which rested on the phloem. The phloem was exposed by incising ~3 mm of the outer-bark with a scalpel (see Chan et al. (2016) for further details). This study used D_x and inner-bark radial variation (D_b). D_b was calculated as the difference between D_w and D_x. D_b, then, includes the phloem tissue produced to the outside of the pre-existing xylem tissue, the vascular cambium and newly formed xylem.

Estimation of radial stem growth

Radial stem variation arises due to three main processes: irreversible cambial growth, a reversible xylem water potential-induced change and a reversible osmotic concentration change (Sevanto et al. 2003, Daudet et al. 2005, Mencuccini et al. 2013). We separated the transpiration-driven, xylem water potential-induced change (derived from xylem radial variation) from measured inner-bark (derived from dendrometer data), to reveal the variations caused by osmotic concentration and cambial growth (Chan et al. 2016). This approach applies Hooke's Law, where water-related changes in the xylem radius reflected changes in xylem water potential (Perämäki et al. 2001). Accordingly (in the absence of any other influences), the inner-bark would also follow xylem water-related changes, tending towards equilibrium. Therefore, the predicted change of the measured inner-bark radius ($\hat{D}_b$) that is solely affected by xylem water potential, at time ($t + \Delta t$) (i.e., the next measuring point), can be predicted from the changes in inner-bark and xylem radii at time (t) (Mencuccini et al. 2013, Chan et al. 2016):

$$\hat{D}_b(t + \Delta t) = \hat{D}_b(t) + \alpha(\beta \Delta D_x(t) - \hat{D}_b(t))\Delta t, \quad (1)$$

where ΔD_x is the measured radial change in xylem radius, α is the radial hydraulic conductance between the xylem and inner-bark and β is the ratio of the elastic modulus of the inner-bark to xylem (for a given change in xylem potential). Parameters α and β were estimated by employing a non-linear, least-square regression fitting over Eq. (1) using inner-bark and xylem measurements at 30-min intervals, over the whole sampling period (Excel Solver, Microsoft, USA). The difference between the measured inner-bark radius (ΔD_b) and $\hat{D}_b$ is the variation that is not explained by the xylem water potential ($\hat{\Delta} G_m$):

$$\hat{\Delta} G_m(t) = \Delta D_b(t) - \hat{\Delta} D_b(t). \quad (2)$$

In other words, $\hat{\Delta} G_m$, expressed in mm, can be used as proxy for volumetric radial stem growth. In reality, $\hat{\Delta} G_m$ also includes influences from reversible osmotic concentration changes of the inner-bark, which we were not able to further separate. However, our previous analysis suggested that the osmotic concentration change effect on $\hat{\Delta} G_m$ would maximally be ~30% on a diurnal scale (Chan et al. 2016). For additional detail in modelling estimation and parameterization, refer to Chan et al. (2016).

Calculation of growth efficiency

The growth efficiency (Y) is a dimensionless coefficient defined as the ratio at which sugar is transformed into new dry mass (ΔW) to the total amount of assimilates required for this transformation to occur, which consists of the sum of the total accumulated growth respiration (R_{ga}) and ΔW of the stem (Thornley 1970, Roux et al. 2001):

$$Y = \frac{\Delta}{(\Delta W + R_{ga})}. \quad (3)$$

Growth efficiency is apparent on a time scale shorter than annual, since the observed growth dynamics are due to the change in volume growth and not accumulated mass. In this study, the accumulated mass (in terms of Y) is of interest, and at the annual scale, the volume and accumulated mass should be linearly proportional to one another, provided that wood density stays constant (which is assumed). However, it is expected that biomass accumulation continues after radial width increment ceases, and likely at a higher rate due to the accumulation of thick-walled latewood (Cuny et al. 2015).

ΔW is observed as the amount of carbon content-per-wood volume per unit length $\left(\rho_{\frac{carbon_{content}}{wood_{volume}}}\right)$ within a certain change in volume of stem per unit length (ΔV):

$$\Delta W = \rho_{\frac{carbon_{content}}{wood_{volume}}} \Delta V. \quad (4)$$

For Scots pine, it is estimated that $\rho_{\frac{carbon_{content}}{wood_{volume}}}$ is ~220 kg m^{-3}. ΔV can further be expressed as

$$\Delta V \approx 2\pi r \Delta d \approx \pi d \Delta d, \quad (5)$$

where d is the diameter of the tree and Δd is maximum $\hat{\Delta} G_m$ after the growing season. From this equation, Eq. (6) can be rewritten to express the change in volume as the change in inner-bark diameter (for 1 m length of stem):

$$\Delta W = \rho_{\frac{carbon_{content}}{wood_{volume}}} \pi d \Delta d. \quad (6)$$

For estimation of Y, we assume that developing wood has the same density as mature wood. Although the intra-annual density

between earlywood and latewood varies, the relative difference is subtle (Jyske et al. 2008). Y was calculated annually and for the second and third phases of each year (see Statistical analysis section for phase separation). It was not calculated for the first phase since appreciable radial growth did not yet readily occur. Due to insufficient E_S data for one tree in 2015 (~41 days missing), calculation of Y for this tree was not possible.

Stem CO₂ efflux measurements

Stem CO_2 efflux (E_S), expressed as µg CO_2 m^{-2} s^{-1}, was measured using an automated chamber system comprising of an acrylic chamber (height 20 cm and width 3.5 cm) attached to the bark of the tree (Kolari et al. 2009). A continuous flow of 1.3 l min^{-1} through the system was applied to measure stem CO_2 efflux. Within the chamber, the efflux was measured as the difference between the CO_2 concentration of the ambient air into the system and the CO_2 concentration flowing out from the system. The chamber system was installed at a height of 12 m in 2007 and moved to 11.4 m (25 June) in 2008 due to technical maintenance. In 2009, measurement height was at 14.1 m. In 2011 (13 July), the continuous flow was adjusted to 1.1 l min^{-1} due to further technical diagnostics.

Measured E_S does not wholly represent all locally respired CO_2 (Trumbore et al. 2013). It could differ due to (i) the release of CO_2 from other parts of the tree that has been transported upwards in xylem water; (ii) the removal of CO_2 by the transpiration stream; and (iii) the release of CO_2 in xylem storage pools (Hölttä and Kolari 2009, Ubierna et al. 2009). To limit the influence of (i) and (ii) for this study, night-time stem respiration rates (22:00–05:00 h) were used in order to capture CO_2 efflux that had not been significantly affected by axial convection of respired CO_2 along with xylem sap flow. Although sap flow may occur during the night, it has been shown to be small (Daley and Phillips 2006). The contribution from the release of CO_2 in xylem storage pools to measured E_S was found to be negligible (McGuire and Teskey 2004, Saveyn et al. 2008) and thus omitted in this study.

An exponential equation was used to describe the temperature response of woody tissue respiration (R):

$$R = E_{S10} \times Q_{10}^{(10-T)/10}, \tag{7}$$

where E_{S10} is the CO_2 efflux at a tissue temperature of 10 °C, Q_{10} is the temperature coefficient of respiration and T is the lagged temperature at reference point R. Studies have found an acclimation response of respiration to the seasonal variation in temperature (Atkin and Tjoelker 2003). In this study, respiration followed temperature with a time lag of no more than 2 h, which is due to a diffusion resistance to movement of CO_2 from the stem to air (Ryan et al. 1995, Lavigne et al. 1996). To compensate for this lagged response; respiration was regressed against prior temperature of 1.5 h as it gave the best fit.

To calculate annual maintenance respiration rates (R_m), Q_{10} was calculated over a continuous interval of 2 weeks during a period of non-growth activity (i.e., 2 weeks before DOY 130 or 2 weeks after DOY 240). It is assumed that during this period, E_S was caused solely by the maintenance respiration component, and that changes due to temperature would also reflect similar changes during the growing season. Thus, Q_{10} and E_{S10} parameter values derived from the non-growing period were used with Eq. (3) to estimate R_m (µg CO_2 m^{-2} s^{-1}).

Q_{10} was calculated separately for each dataset using the following equation and the value obtained was inserted into Eq. (3):

$$Q_{10} = \left(\frac{R_2}{R_1}\right)^{\frac{10}{T_2-T_1}}, \tag{8}$$

where R_1 and R_2 are CO_2 efflux rates at temperatures T_1 and T_2. Growth respiration rate (R_g; µg CO_2 m^{-2} s^{-1}) was then calculated as the difference between R_m and measured total stem CO_2 efflux (E_S).

Statistical analysis

To fully capture the summer growing season, this study used 30-min mean values from 1 April to 5 October for the years 2007–09, 2011 and 2015. Field-collected radial stem variations and $\hat{\Delta}G_m$ were set to zero on 1 April of each year as this date precedes the beginning of the growing season. Intra-annual tree growth was divided into three distinct phases: the first phase was defined as the period from 1 April to the date when the first tracheids were observed from microcores (8 June, 29 May and 28 May in 2007, 2008 and 2009, respectively; refer to Chan et al. (2016) for reference and microcore sampling method). No microcore samples were taken in 2011 and 2015, so an estimate was made based on observations from previously sampled years as to when the first tracheids may have been formed. The second phase was defined as the period from the end of the first phase to the date when a significant decline of SGR occurred, based on a calculated moving average of 10 days (25 July, 7 August, 2 August, 1 August and 20 July for years 2007, 2008, 2009, 2011 and 2015, respectively) derived from dendrometers. The third phase was defined as the period from the end of the second phase to 5 October.

For some analyses, daily mean values were calculated for R_g, temperature and $\hat{\Delta}G_m$. In addition, the daily derivatives of $\hat{\Delta}G_m$ ($\Delta\hat{\Delta}G_m$; mm day^{-1}) and raw whole-stem radial variation (ΔD_w; mm day^{-1}) were calculated (i.e., the difference between two consecutive daily maximum values) and represented as daily SGR. Cross-correlation analysis was performed for each year between daily R_g to each daily SGR series to reveal any time lag, and adjusted to this lag when performing coefficient of determination analyses (r^2) between R_g to each daily SGR series. All r^2 analyses were performed using linear regression (SPSS v23). For manuscript readability, $\hat{\Delta}G_m$ will hereafter be called modelled

growth (accumulated growth over the whole season); $\Delta\hat{\Delta}G_m$, modelled daily growth (daily growth rate); ΔD_w, raw growth (accumulated growth over the whole season, the raw dendrometer signal); and $\Delta\Delta D_w$, raw daily growth (daily growth rate, the raw dendrometer signal). Since partitioning respiration into growth and maintenance respiration component is not unambiguous and straightforward (e.g., Ryan et al. 2009), we also conducted a parallel analysis (see Supplementary Data at *Tree Physiology* Online) where we did not partition respiration into growth vs maintenance respiration, but simply compared growth against respiration, i.e., using E_S in place of R_g.

To compare the temporal variability in the relationship between R_g to both temperature and GPP, we used wavelet analysis, specifically continuous wavelet transform (CWT) and wavelet coherence (WC) analysis using the wavelet toolbox (Grinsted et al. 2004) in Matlab R2016a. Previous studies have described wavelet analysis in detail (Torrence and Compo 1998, Grinsted et al. 2004, Vargas et al. 2011, Gea-Izquierdo et al. 2015, Natalini et al. 2016). Continuous wavelet transform identifies the common period in the time–frequency space. Meanwhile, WC analysis identifies the coherence (high and low)—i.e., the measured linear dependency between two series, by testing for similar frequency components (Torrence and Compo 1998). Wavelet coherence analysis is used because it allows for detection of phase differences (i.e., time lags) and its variation between the two series over time, and thus, time lags can be determined at each period where high coherence is found (Vargas et al. 2011). For each wavelet analysis, the 5% significance level and edge effects were calculated.

Results

Measured and modelled radial growth sampling

Measured xylem radial variation (D_x) showed a consistent diurnal pattern during the course of the growing season for all years – shrinking due to transpiration during the day, and swelling during the night without any major change in the minimum and maximum values (refer to Figure 4 in Chan et al. (2016)). Raw growth (D_w) over the same time course had a similar diurnal pattern, and on a seasonal scale, a sigmoidal increase. This increase exhibited an exponential rise of the daily maximum value in the early summer, a phase of linear increase after mid-July, and reaching its seasonal maximum radius in mid-August before declining slightly shortly after in late September (not shown). As expected, modelled growth showed a high correlation to raw growth in all years over the whole growing season (not shown)—modelled growth began approximately at the same time as raw growth increment (week 20/21) and reached its seasonal peak in growth in late July/early August. Water-related changes, as seen in raw growth, masked observable growth on the sub-diurnal scale and on a diurnal scale during (and shortly after) precipitation events. During these precipitation events, the stem swelled considerably until the rains had

subsided. Modelled daily growth ($\Delta\hat{\Delta}G_m$) increased from late May to late June, when rapid development of stem growth occurred in all years (Figure 1; see Figure S1 available as Supplementary Data at *Tree Physiology* Online). After this rapid increase, modelled daily growth declined rapidly at the beginning of July from years 2007 to 2009 and 2015, and on 20 July in 2011. After August, modelled daily growth decline was further pronounced, with a SGR below zero at the end of the measurement period. Remarkably, the patterns of modelled daily growth of the two trees in 2015 were very similar.

Relation of stem CO$_2$ efflux to stem growth

Observed stem CO_2 efflux rates (E_S) had a close exponential relationship with air temperature throughout the study period. During the night (22:00–05:00 h), E_S and temperature correlations showed a year-to-year r^2 range from 0.62 to 0.85, and had a considerably higher r^2 than day-time values (07:00–19:00 h), which ranged from 0.59 to 0.80 (Figure 2). As in typical boreal environments, periods before May and after September had lower Q_{10} values (1.31–1.46) than summer (June–August) Q_{10} values (1.92–2.07).

Generally, R_m was much smaller and less variable in comparison with R_g over the whole growing season, in all years (Figure 1). R_g corresponded with changes in E_S, with transient growth respiration activity already occurring as early as the first week of April. In late May, R_g increased rapidly in comparison with R_m, and maintained this high rate until late August. In late August, R_g began to decline steadily to springtime levels.

To correlate the daily SGR series (i.e., modelled daily growth and raw daily growth) to R_g, the daily mean values of R_g were regressed against each daily SGR series and separated into three growth phases: first, second and third (Figure 1). A cross-correlation function of R_g to each daily SGR series covering the second and third phases revealed a 1-day time lag of R_g to modelled daily growth (Figure 3) and no correlation to raw daily growth ΔD_w (not shown). Therefore, for further growth analyses, the results were adjusted for a 1-day time lag. R_g-modelled daily growth correlation analyses yielded similar phase-to-phase characteristics for each year (Table 3). A cross-correlation analysis was also performed between E_S and modelled daily growth (i.e., without separation of respiration to maintenance and growth respiration), which showed qualitatively similar results, but revealed a bit less consistency than that of R_g to modelled daily growth (see Figure S2 available as Supplementary Data at *Tree Physiology* Online). The first phase showed no consistent R_g-modelled daily growth correlation. However, a significant r^2 was found in the second and third phases (except for the latter in 2011), with the second phase showing higher correlation ($P < 0.01$). On average, the second phase explained ~30% of total R_g variation and showed ~50% higher correlation than the third phase, which explained ~15% of total R_g variation. R_g-raw daily growth correlation revealed inconsistencies year-to-year during the second
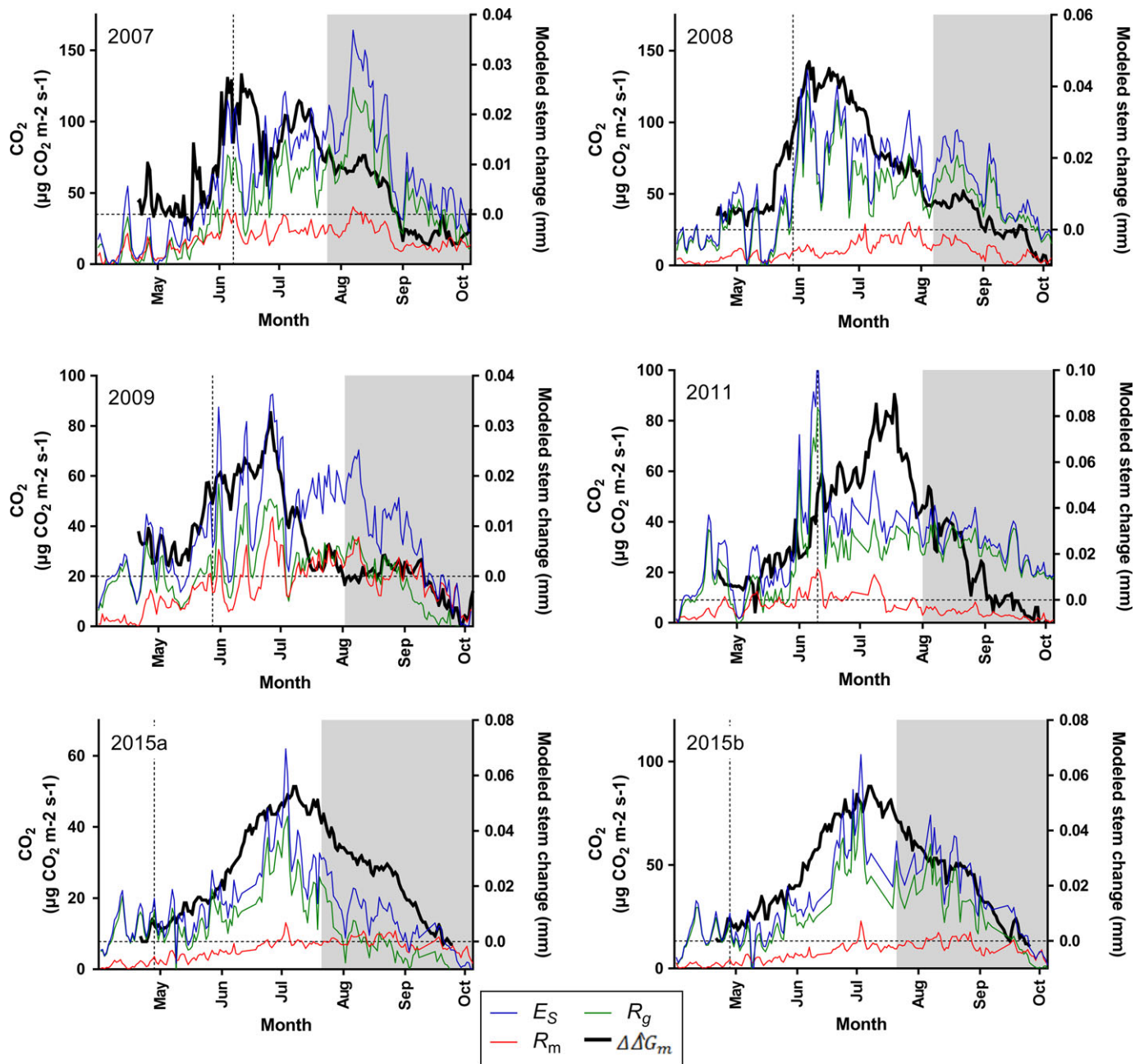
Figure 1. Daily intervals of stem CO_2 efflux (E_S, blue), maintenance respiration (R_m, red) and growth respiration (R_g, green). The dotted, vertical black line denotes the first observation of tracheid formation (i.e., beginning of the second phase) from measured microcores. The dotted, horizontal line denotes the zero point of the daily growth rate derived from the model ($\Delta\hat{\Delta}G_m$). $\Delta\hat{\Delta}G_m$ (black) was averaged over 10 days to determine the third phase (grey shade). However, all correlation analyses in this study used daily (non-averaged) values.

phase compared with R_g-modelled daily growth correlation. In this phase, R_g-raw daily growth showed high correlation in 2011 and 2015a ($P < 0.01$), a low correlation in 2008 and 2015b, and no correlation in 2007 and 2009. The r^2 significance values of R_g-raw daily growth correlations in the third phase were not as consistent compared with those of R_g-modelled daily growth correlations. The correlation between modelled daily growth rate and E_S showed very similar results to that of R_g-modelled daily growth

correlations for each phase and all years (see Table S1 available as Supplementary Data at *Tree Physiology* Online).

Growth efficiency

The growth efficiency (Y) estimated for the whole growing season varied from 0.64 to 0.81 (Table 4). Apparent (i.e., intra-annual) Y was higher during the second phase and declined during the
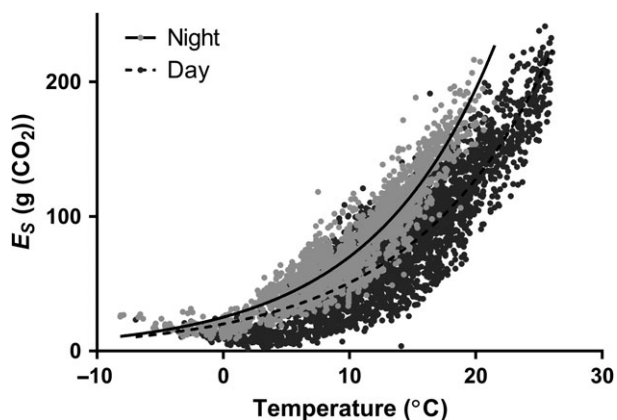
Figure 2. Regression between stem CO_2 efflux (E_S) and temperature during the day (07:00–19:00 h, dark grey) and night (22:00 and 05:00 h, light grey) at half-hourly intervals with their respective exponential fitted curve from 1 April to 5 October 2007. Figure has been corrected with a 1.5 h temperature lag to E_S.
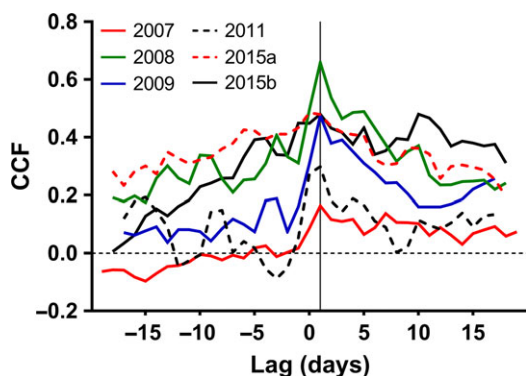

Figure 3. Cross-correlation function (CCF) of daily-averaged, night-time values of growth respiration (R_g) to modelled daily growth rate ($\Delta\hat\Delta G_m$) for all years studied. Dotted horizontal line indicates zero point. Vertical solid line indicates period with highest correlation.

third phase, although only slightly for 2015a. The highest estimated apparent Y during the second phase was seen in 2008, followed by 2009 and for 2015a. Meanwhile, apparent Y in the third phase of 2007 was lower than the other years, with 2015a showing the highest. In 2008, there was significantly more apparent biomass growth than the other years in the second phase. The apparent biomass growth was reduced considerably during the third phase, with 2008 showing the least apparent biomass growth. Apparent biomass growth in the third phase decreased more than 90% compared with their respective second phase's apparent biomass growth except in 2015, which decreased only 59%.

Connection between growth respiration, GPP and temperature

Since all years observed yielded similar results from both continuous wavelet transform (CWT) and wavelet coherence (WC) analysis, we have focused on the year 2009 in the manuscript. Figures for other

Table 3. Squared correlation coefficient (r^2) between growth respiration (R_g) and the modelled daily growth rate ($\Delta\hat\Delta G_m$) and raw daily growth rate (ΔD_w). Intra-annual growth was separated into phases that represented predominant growth processes. Phase 1 is from 1 April to the date when tracheids were first observed; Phase 2 was the period from the end of Phase 1 to a day when significant decline of growth rate occurred; and Phase 3 was the period from the end of Phase 2 to 5 October, when growth has stopped.

	Measurement	Phase 1	Phase 2	Phase 3
2007	$\Delta\hat\Delta G_m$	0.05*	0.30**	0.16**
	ΔD_w	0.02	0.00	0.04
2008	$\Delta\hat\Delta G_m$	0.02	0.36**	0.15**
	ΔD_w	0.08*	0.05*	0.03
2009	$\Delta\hat\Delta G_m$	0.04	0.25**	0.15**
	ΔD_w	0.00	0.01	0.00
2011	$\Delta\hat\Delta G_m$	0.01	0.31**	0.01
	ΔD_w	0.00	0.31**	0.04
2015a	$\Delta\hat\Delta G_m$	0.04	0.30**	0.18**
	ΔD_w	0.00	0.16**	0.05
2015b	$\Delta\hat\Delta G_m$	0.01	0.22**	0.17**
	ΔD_w	0.08*	0.11*	0.04

Significant levels at 0.05 and 0.01 are indicated by * and **, respectively.

years can be found in the Supplementary Data at *Tree Physiology* Online. Continuous wavelet transform of R_g, GPP and temperature variables each revealed a significance at a period of 1 day, indicating a common diurnal pattern (Figure 4; see Figures S3–S6 available as Supplementary Data at *Tree Physiology* Online). From May onwards of 2009, GPP revealed a significance at the 5% level, which ended at the end of October. R_g indicated sporadic significance from May to mid-June, and from that point onwards, constant significance until early September. Meanwhile, temperature showed continual significance throughout the 2009 year.

Wavelet coherence analysis showed the strongest coherence of R_g, to both GPP and temperature at a period of 1 day for all years (Figure 5; see Figures S7–S11 available as Supplementary Data at *Tree Physiology* Online). There was also evidence for sporadic significant coherence at higher frequencies (<1 day). In 2009, significant coherence was found from late April to October; coherence was also observed earlier, but it was not consistent. Coherence at higher frequencies were almost absent in R_g-GPP analysis, but consistent in R_g-temperature analysis. Time lags differed throughout the season. For example, R_g-GPP analysis in 2009 (Figure 5a) revealed a time lag of ~6 h (R_g following GPP) in the spring, but during the remainder of the growing season, the R_g-GPP lag was ~3 h. R_g-temperature WC analysis however, revealed a much smaller lag (~1–2 h).

Discussion

As shown by our results, raw dendrometer measurements used as proxy for volumetric stem growth cannot be scaled for short-term (e.g., daily) observations. This is because non-growth signals

Table 4. Growth efficiency (Y), apparent biomass growth (g (C)), annual biomass growth (g (C)) and growth respiration (g (C)) were calculated for the second (P2) and third (P3) phases. Whole year (annual) was calculated for growth efficiency and biomass growth. Both the apparent and whole year biomass growth and growth respiration values are derived variables for calculating apparent Y and annual Y, respectively. Annual Y and annual biomass growth include first phase values. 2015b was omitted due to insufficient data.

Year	Apparent Y		Annual Y	Apparent biomass growth		Annual biomass growth	Growth respiration	
	P2	P3		P2	P3		P2	P3
2007	0.65	0.10	0.70	89.59	6.47	179.55	47.57	67.46
2008	0.81	0.14	0.81	233.71	2.77	328.72	53.57	16.59
2009	0.78	0.31	0.74	110.59	5.42	195.89	30.91	12.12
2011	0.72	0.32	0.64	65.56	11.91	98.17	26.98	25.91
2015a	0.73	0.70	0.71	70.07	28.56	100.73	26.29	12.04
2015b	–	–	–	–	–	–	–	–

*($P < 0.05$), **($P < 0.01$).

(e.g., water-related processes) are also observed from these measurements (Bäucker et al. 1998, Sevanto et al. 2011, Mencuccini et al. 2013, 2017, Chan et al. 2016, Zweifel 2016). Representing growth with the inclusion of these undesired signals may pose great challenges, as these signals generally prevail over desired signals (i.e., growth), particularly on the daily scale. By isolating these water status-related signals from raw dendrometer data and then analysing the solely growth-related signals, further in-depth investigation of growth is possible. However, our results indicate that partitioning measured E_S into functional components of growth and maintenance respiration is not wholly necessary, but may aid in complex respiration studies.

Previous studies such as Stockfors and Linder (1998) and Vose and Ryan (2002) used ΔD_w for their analyses, and to counter-act the deficiencies from using such measurements, selected dates or long intervals were used, respectively. Although direct comparison between the results from this study and previous studies may appear counter-intuitive, it draws attention to the importance of the separation of growth-related variations from water-induced changes found from dendrometer measurements.

Using the mature tissue method to separate E_S into maintenance respiration rate (R_m) and growth respiration rate (R_g) components revealed a relatively small and constant R_m during the growing season in comparison with growth respiration (R_g) (Figure 1). To confirm the relation between growth and respiration, we conducted an additional analysis where we did not separate E_S into maintenance and growth components, and the results were similar to results using the mature tissue method (see Figure S1, Table S1 available as Supplementary Data at *Tree Physiology* Online).

Link between growth respiration and stem growth

After separating intra-annual growth into phenological phases, R_g was compared with the modelled daily growth rates of $\hat{\Delta}G_m$ ($\Delta\hat{\Delta}G_m$) and raw daily growth rates (ΔD_w). R_g-raw daily growth correlations revealed a lack of consistency within-year and year-to-year (Table 3). This contrasted R_g-modelled daily growth

correlations, which showed comparable inter- and intra-annual dynamics. The dynamics of R_g-modelled daily growth were similar to studies from Stockfors and Linder (1998) in *Picea abies* and Vose and Ryan (2002) in *Pinus strobus*, where they found a low correlation during the spring (first phase), increasing greatly during the summer rapid-growth period (second phase), and slightly decreasing when growth has slowed (third phase).

It is anticipated that the first phase would yield low correlation since growth was minimal during this phase. However, R_g revealed rapid, transient increases beginning 2 weeks before stem increment and a month before the onset of tracheid formation (Figure 1). Although these increases are more than half of summertime levels, the timing is prior to any tracheid development or observable radial growth, which may indicate metabolic activity due to spring reactivation. Metabolic activity is associated with cambial reactivation (e.g., cambial cell swelling) due to changes in cell biochemistry (Lavigne et al. 2004, Gruber et al. 2009). These observations agree with Lavigne et al. (2004) that the interval between high metabolic activity and xylem production may be several weeks, and may explain the R_g-modelled daily growth correlation for the years 2007 and 2008 ($P < 0.05$). Here, we had microcore reference measurements of the initiation of tracheid formation but it has been reported that the new phloem cells are formed about 10–20 days before xylem cells in Scots pine (Antonova and Stasova 2006). Due to the thin phloem cell layer, death of the previous year's phloem cells and the elasticity of living bark, associated changes in stem radius may remain masked, particularly by the hydraulic variation of the living bark in the spring. Considering this, considerable energy is used for the preparatory phases before the actual onset of tracheid formation/growth.

R_g-modelled daily growth correlations in the second phase were highly significant in all years ($P < 0.01$). This is expected since this phase is characterized by a high rate of cell enlargement and growth concurrently with high photosynthetic activity (Gordon and Larson 1968). Carbohydrate concentration levels can be expected to increase due to photosynthetic activity, which ultimately promotes growth and hence respiration (Ainsworth and Bush 2011). In this phase, R_g-modelled daily growth correlation
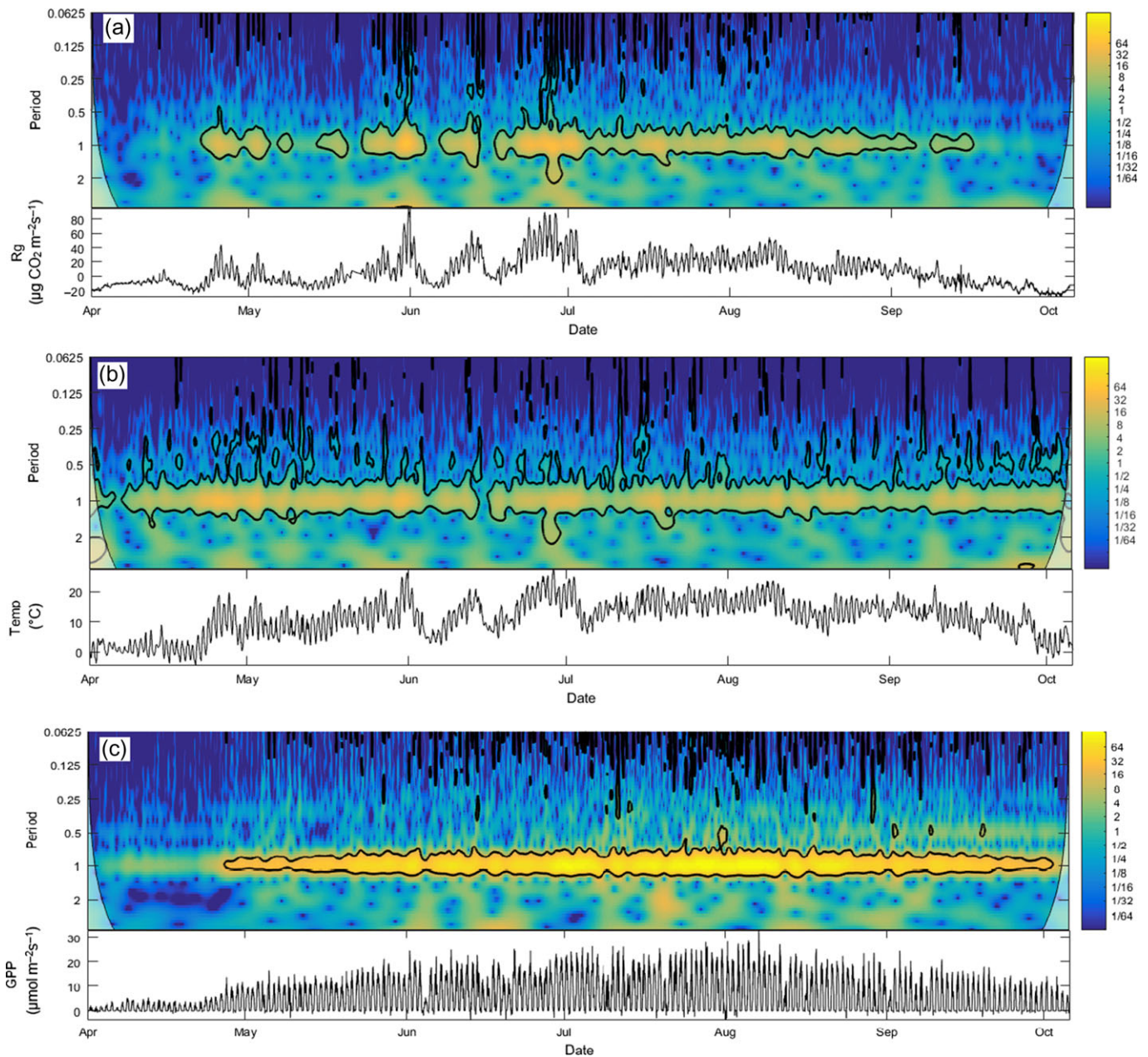
Figure 4. Time series (bottom) and its continuous wavelet analysis (top) of R_g (a), temperature (b) and GPP (c) in 2009 at hour–hour intervals. Within the wavelet analysis figures, the black contour lines indicate the 5% significance level and beyond black lines indicate the cone of influence where edge effects may distort the image. High and low coherence is indicated by the colours yellow and blue, respectively.

had a mean r^2 of 0.31, estimated with daily intervals. This result is similar to *P. strobus* ($r^2 = 0.32$, measured with ~30 day intervals; Vose and Ryan (2002)), but slightly lower than another study with *P. sylvestris* ($r^2 = 0.45$, measured with a mean monthly SGR; Zha et al. (2004)), and considerably lower than *P. abies* ($r^2 = 0.65–0.93$, measured on specific dates; Stockfors and Linder (1998)). There are some factors which may explain the proportion of R_g that was not explained by stem growth. For example, growth derived from dendrometers can only observe cell division and enlargement processes but not cell wall thickening processes. This latter process may occur during the second phase and can

comprise a large proportion of R_g that could not be observed from $\Delta\hat{\Delta}G_m$. Furthermore, CO_2 moves axially with the xylem sap and whether it reduces or increases E_S locally largely depends on vertical location (Hölttä and Kolari 2009). We tried to minimize this effect by looking at only night-time fluxes. Additionally, non-structural carbon supply may have a large effect on stem R_g, as carbon compounds are drawn from the stem reserves to areas required for growth and maintenance (Hoch et al. 2003). Although not quite relevant at this study boreal site, water stress is an environmental factor that affects respiration rates (Flexas et al. 2006). For example, respiration rates increase after a
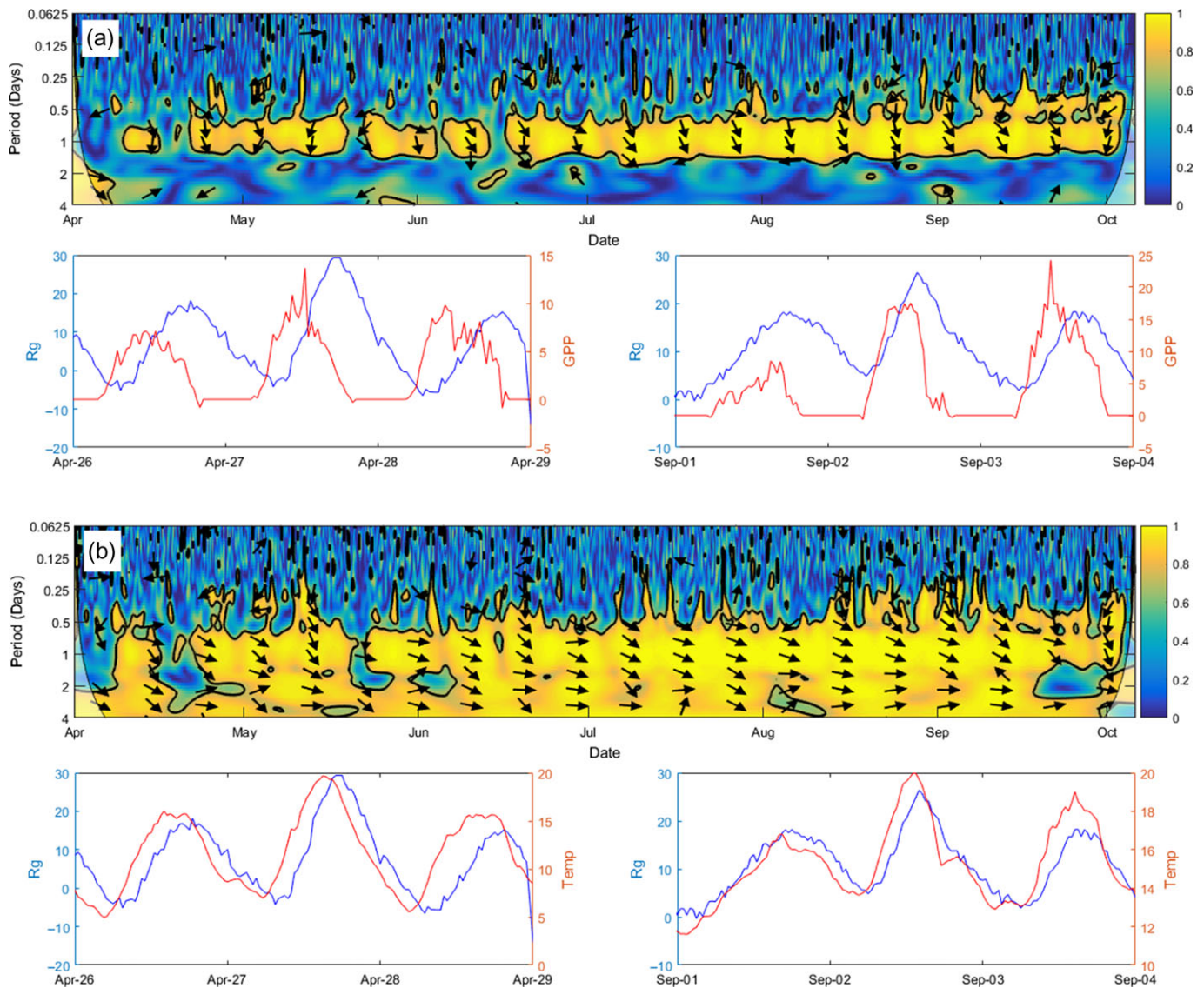
Figure 5. Selected time series and wavelet coherence analysis between R_g and GPP (a) and between R_g and Temperature (b) in 2009 at hour–hour intervals. The black contour lines indicate the 5% significance level and beyond black lines indicate the cone of influence where edge effects may distort the image. The phase difference (i.e., time lag) is shown by arrows (R_g lags behind). Arrows pointing right indicate no lag; down, ~6 h; and left, ~12 h. High and low coherence is indicated by the colours yellow and blue, respectively. Line figures below each WC analysis representing two, 3-day events (26–29 April; 1–4 September) show the diurnal cycle of R_g and GPP (top) and R_g and temperature (bottom). Although WC analysis is bidirectional, the line figures indicate a R_g (blue) lag to GPP and temperature (red). Refer to Table 1 for variable units.

period of water stress—a necessity for photosynthetic recovery (Kirschbaum 1988).

The third phase was characterized by the decrease in cell division and cell enlargement (Deslauriers et al. 2009), and the increase in cell wall thickening processes. As a result, stem growth may not be well represented in this phase compared with the second phase, especially when using raw dendrometer measurements and modelled daily growth. Cell enlargement was observed but at a reduced level since the development of earlywood and latewood cells declined after mid-August. Generally in northern latitudes, volumetric growth reaches its maximum towards the summer solstice before declining (Leikola 1969,

Rossi et al. 2006b). The observed decrease in R_g-modelled daily growth correlation following the second phase follows observations from Vose and Ryan (2002) and Stockfors and Linder (1998). However, all years except for 2011 still showed significant r^2 values. Volumetric growth in 2011 was particularly exceptional as it continued until late July before declining. The small decline in SGR below zero observed at the end of the third phase in all years may be due to the newly formed xylem conduits conducting water, which causes water to be under tension and thus, causing a decrease in stem diameter (Sperry and Sullivan 1992). Another possibility is due to decreasing osmotic strength with decreasing GPP towards autumn.

Lagged responses between growth respiration and growth

An R_g-modelled daily growth cross-correlation analysis revealed a consistent 1-day time lag of modelled daily growth preceding R_g in all years (Figure 3). This may be partly due to within-stem diffusion resistances causing stem CO_2 efflux to lag actual stem respiration. Although not explicitly reported by Hölttä and Kolari (2009), they found that diffusion from within the stem into the atmosphere took ~2.5 h at the study site. It is therefore likely that R_g could escape from the stem to the atmosphere in less than a day. In this study, we have found E_S higher at night (22:00–05:00 h) compared with day-time values (07:00–19:00 h) at comparable temperatures (Figure 2), which may indicate two processes occurring: higher growth activity occurring at night and sap flow affecting E_S during the day. Higher growth activity affecting respiration rates bears an interesting implication on eddy covariance measurements because TER estimation is based solely on night-time values. Therefore, future GPP modelling estimations may have to take this into consideration.

Previous studies on the time lag between respiration and stem growth varied from 1 to 25 days (Zumer 1969) and from 20 to 40 days (Edwards and Hanson 1996). Other studies employed best-fit regression models (Stockfors and Linder 1998, Ceschia et al. 2002), but these have also reported similarly large differences. To contrast, some studies found a correlation with no time lag (Maier 2001, Vose and Ryan 2002, Zha et al. 2004). However, this may be due to having large intervals (e.g., monthly or bi-monthly) or averaging the SGR; which may ultimately mask the lag between respiration and SGR (Maier 2001).

Growth efficiency

Growth efficiency (Y) estimated from April to October ranged from 0.64 to 0.81 (Table 4). This is within the scope of a modelling study from Roux et al. (2001) that analysed over 10 carbon-based models of tree growth, with a reported mean Y of 0.75. Apparent Y revealed similarities year-to-year except for 2015a. In the second phase, the mean apparent Y was ~0.74, and declined ~46% to ~0.22 in the third phase. For 2015a however, apparent Y in the third phase was as high as its second phase. This is because the SGR did not decline as suddenly as in the other years (Figure 1). Generally, the large contrast between these two phases may be due to differences in the allocation of carbon. Much of the carbon in the second phase was apportioned to volumetric increase (e.g., cell enlargement). This observation would further support the high R_g-modelled daily growth correlation observed during this phase. In the third phase, apparent Y estimates showed an apparent decline in new structural development. However, it is clear that R_g remains rather high (Figure 1). Therefore, the proportion of R_g not explained by apparent Y and R_g-modelled daily growth dynamics may be due to secondary thickening and deposition of new materials (e.g., cellulose, lignin and cutin) (Gričar et al. 2005,

Rossi et al. 2006a) and not detectable by radial stem measurements.

Link between R_g and both GPP and temperature

Since all variables analysed with the wavelet analysis exhibited similar patterns, the interpretation of the analysis is not straightforward. Unlike the r^2 analyses in this study, the current wavelet analysis requires day-time values of R_g to conduct the analysis. While night-time values were uniquely used in the other analyses of this study, day values were used for the wavelet analysis as continuous data is required for it. Therefore, this analysis should be taken with caution as the transport of CO_2 with the xylem sap has not been taken into account. The WC analysis between R_g and other variables showed a significant coherence at the period of one day, demonstrating a common daily cycle and tight correlation between these measured variables. However, it is important to remember that this does not necessarily indicate causality, although it would be tempting to conclude that variations in GPP and recently photosynthetically fixed carbohydrates were causing variation in R_g (Figure 5); as has been shown, e.g., in Zha et al. (2004). The R_g-GPP time lag of ~3 h corresponds to the time scale of sugar concentration propagation rate in the phloem between the foliage and the stem (Mencuccini et al. 2013), and the R_g-temperature time lag of ~2 h corresponds to the time scale of the radial diffusion of respired CO_2 out from the stem. From the same study site for the same species, the R_g-temperature time lag is similar to the result from (Hölttä and Kolari 2009). In mid-April, coherence was found between both GPP and temperature with R_g. This finding correlates well with the results found from R_g-modelled daily growth correlations during the first phase, which may indicate metabolic activity due to spring reactivation.

Conclusions

Our study has demonstrated that dendrometers are powerful instruments to study the stem growth of trees provided that the reversible daily variations in stem water status are accounted for. By using dendrometer measurements in conjunction with other physiological measurements, we are able to link whole-tree physiological processes. In this study, a significant correlation was found between stem growth and stem CO_2 efflux. As a first, we were able to study the relationships between stem growth, GPP and growth respiration on a daily time scale over the course of the growing season and over several years. This analysis revealed two important physiological observations: that the relationship between R_g and growth differed substantially at different times of the year, and that there was a consistent 1-day time lag of R_g to growth. This study demonstrates the need for further in-depth analysis of growth and respiration dynamics—especially pertaining to cellular respiration at specific developmental stages, its woody tissue costs and linkages to source–sink processes.

Supplementary Data

Acknowledgments

Conflict of interest

None declared.

Funding

References

Ainsworth EA, Bush DR (2011) Carbohydrate export from the leaf: a highly regulated process and target to enhance photosynthesis and productivity. Plant Physiol 155:64–69.

Amthor JS (1989) Respiration and crop productivity. Springer, New York, p 215.

Antonova G, Stasova V (2006) Seasonal development of phloem in Scots pine stems. Russ J Dev Biol 37:306–320.

Araki MG, Kajimoto T, Han Q, Kawasaki T, Utsugi H, Gyokusen K, Chiba Y (2015) Effect of stem radial growth on seasonal and spatial variations in stem CO2 efflux of *Chamaecyparis obtusa*. Trees 29:499–514.

Asshoff R, Zotz G, Koerner C (2006) Growth and phenology of mature temperate forest trees in elevated CO2. Glob Chang Biol 12: 848–861.

Atkin OK, Tjoelker MG (2003) Thermal acclimation and the dynamic response of plant respiration to temperature. Trends Plant Sci 8:343–351.

Bäucker E, Bues C-T, Vogel M (1998) Radial growth dynamics of spruce (*Picea abies*) measured by micro-cores. IAWA J 19:301–309.

Bloemen J, McGuire MA, Aubrey DP, Teskey RO, Steppe K (2013) Transport of root-respired CO_2 via the transpiration stream affects aboveground carbon assimilation and CO2 efflux in trees. New Phytol 197:555–565.

Bowman WP, Barbour MM, Turnbull MH, Tissue DT, Whitehead D, Griffin KL (2005) Sap flow rates and sapwood density are critical factors in within-and between-tree variation in CO2 efflux from stems of mature *Dacrydium cupressinum* trees. New Phytol 167:815–828.

Brito P, Morales D, Wieser G, Jiménez MS (2010) Spatial and seasonal variations in stem CO2 efflux of *Pinus canariensis* at their upper distribution limit. Trees 24:523–531.

Cajander AK (1909) Ueber Waldtypen. Acta For Fenn 1:1–176.

Carey EV, DeLucia EH, Ball JT (1996) Stem maintenance and construction respiration in *Pinus ponderosa* grown in different concentrations of atmospheric CO2. Tree Physiol 16:125–130.

Ceschia É, Damesin C, Lebaube S, Pontailler J-Y, Dufrêne É (2002) Spatial and seasonal variations in stem respiration of beech trees (*Fagus sylvatica*). Ann For Sci 59:801–812.

Chan T, Hölttä T, Berninger F, Mäkinen H, Nöjd P, Mencuccini M, Nikinmaa E (2016) Separating water-potential induced swelling and shrinking from measured radial stem variations reveals a cambial growth and osmotic concentration signal. Plant Cell Environ 39:233–244.

Cuny HE, Rathgeber Cyrille B, Frank D et al. (2015) Woody biomass production lags stem-girth increase by over one month in coniferous forests. Nat Plants 1:1–6.

Daley MJ, Phillips NG (2006) Interspecific variation in nighttime transpiration and stomatal conductance in a mixed New England deciduous forest. Tree Physiol 26:411.

Daudet F-A, Améglio T, Cochard H, Archilla O, Lacointe A (2005) Experimental analysis of the role of water and carbon in tree stem diameter variations. J Exp Bot 56:135–144.

Desai AR, Richardson AD, Moffat AM et al. (2008) Cross-site evaluation of eddy covariance GPP and RE decomposition techniques. Agric For Meteorol 148:821–838.

Deslauriers A, Rossi S, Anfodillo T (2007) Dendrometer and intra-annual tree growth: what kind of information can be inferred? Dendrochronologia 25:113–124.

Deslauriers A, Giovannelli A, Rossi S, Castro G, Fragnelli G, Traversi L (2009) Intra-annual cambial activity and carbon availability in stem of poplar. Tree Physiol 29:1223–1235.

Edwards NT, Hanson PJ (1996) Stem respiration in a closed-canopy upland oak forest. Tree Physiol 16:433–439.

Flexas J, Bota J, Galmes J, Medrano H, Ribas-Carbó M (2006) Keeping a positive carbon balance under adverse conditions: responses of photosynthesis and respiration to water stress. Physiol Plant 127: 343–352.

Gansert D, Burgdorf M (2005) Effects of xylem sap flow on carbon dioxide efflux from stems of birch (*Betula pendula* Roth). Flora-Morphol Distrib Funct Ecol Plants 200:444–455.

Gea-Izquierdo G, Montes F, Gavilán R, Cañellas I, Rubio A (2015) Is this the end? Dynamics of a relict stand from pervasively deforested ancient Iberian pine forests. Eur J For Res 134:525–536.

Gordon JC, Larson PR (1968) Seasonal course of photosynthesis, respiration, and distribution of 14C in young *Pinus resinosa* trees as related to wood formation. Plant Physiol 43:1617–1624.

Goulden ML, McMillan A, Winston G, Rocha A, Manies K, Harden JW, Bond-Lamberty B (2011) Patterns of NPP, GPP, respiration, and NEP during boreal forest succession. Glob Chang Biol 17:855–871.

Gričar J, Čufar K, Oven P, Schmitt U (2005) Differentiation of terminal latewood tracheids in silver fir trees during autumn. Ann Bot 95: 959–965.

Grinsted A, Moore JC, Jevrejeva S (2004) Application of the cross wavelet transform and wavelet coherence to geophysical time series. Nonlin Process Geophys 11:561–566.

Gruber A, Wieser G, Oberhuber W (2009) Intra-annual dynamics of stem CO2 efflux in relation to cambial activity and xylem development in *Pinus cembra*. Tree Physiol 29:641–649.

Hoch G, Richter A, Körner C (2003) Non-structural carbon compounds in temperate forest trees. Plant Cell Environ 26:1067–1081.

Hölttä T, Kolari P (2009) Interpretation of stem CO2 efflux measurements. Tree Physiol 29:1447–1456.

Jyske T, Mäkinen H, Saranpää P (2008) Wood density within Norway spruce stems. Silva Fenn 42:439–455.

Kirschbaum M (1988) Recovery of photosynthesis from water stress in *Eucalyptus pauciflora*—a process in two stages. Plant Cell Environ 11: 685–694.

Kolari P, Kulmala L, Pumpanen J, Launiainen S, Ilvesniemi H, Hari P, Nikinmaa E (2009) CO_2 exchange and component CO_2 fluxes of a boreal Scots pine forest. Boreal Environ Res 14:761–783.

Lavigne M, Ryan M (1997) Growth and maintenance respiration rates of aspen, black spruce and jack pine stems at northern and southern BOREAS sites. Tree Physiol 17:543–551.

Lavigne M, Little C, Riding R (2004) Changes in stem respiration rate during cambial reactivation can be used to refine estimates of growth and maintenance respiration. New Phytol 162:81–93.

Lavigne MB, Franklin SE, Hunt ER (1996) Estimating stem maintenance respiration rates of dissimilar balsam fir stands. Tree Physiol 16: 687–695.

Leikola M (1969) The influence of environmental factors on the diameter growth of young trees. Acta For Fenn 92:1–44.

Loveys B, Scheurwater I, Pons T, Fitter A, Atkin O (2002) Growth temperature influences the underlying components of relative growth rate: an investigation using inherently fast-and slow-growing plant species. Plant Cell Environ 25:975–988.

Maier CA (2001) Stem growth and respiration in loblolly pine plantations differing in soil resource availability. Tree Physiol 21:1183–1193.

Maier CA, Johnsen KH, Clinton BD, Ludovici KH (2010) Relationships between stem CO2 efflux, substrate supply, and growth in young loblolly pine trees. New Phytol 185:502–513.

Mäkinen H, Seo J-W, Nöjd P, Schmitt U, Jalkanen R (2008) Seasonal dynamics of wood formation: a comparison between pinning, microcoring and dendrometer measurements. Eur J For Res 127:235–245.

Maunoury-Danger F, Fresneau C, Eglin T, Berveiller D, François C, Lelarge-Trouverie C, Damesin C (2010) Impact of carbohydrate supply on stem growth, wood and respired CO2 δ13C: assessment by experimental girdling. Tree Physiol 30:818–830.

McGuire M, Teskey R (2004) Estimating stem respiration in trees by a mass balance approach that accounts for internal and external fluxes of CO2. Tree Physiol 24:571–578.

Mencuccini M, Hölttä T, Sevanto S, Nikinmaa E (2013) Concurrent measurements of change in the bark and xylem diameters of trees reveal a phloem-generated turgor signal. New Phytol 198:1143–1154.

Mencuccini M, Salmon Y, Mitchell P et al. (2017) An empirical method that separates irreversible stem radial growth from bark water content changes in trees: theory and case studies. Plant Cell Environ 40: 290–303.

Natalini F, Alejano R, Vázquez-Piqué J, Cañellas I, Gea-Izquierdo G (2016) The role of climate change in the widespread mortality of holm oak in open woodlands of Southwestern Spain. Dendrochronologia 38:51–60.

Negisi K (1975) Diurnal fluctuation of CO2 released from the stem bark of standing young Pinus densiflora trees. J Jpn Forestry Soc 57:375–383.

Negisti K (1972) Diurnal fluctuation of CO2 release from the bark of a standing Magnolia obvata tree. J Jpn Forestry Soc 54:257–263.

Perämäki M, Nikinmaa E, Sevanto S, Ilvesniemi H, Siivola E, Hari P, Vesala T (2001) Tree stem diameter variations and transpiration in Scots pine: an analysis using a dynamic sap flow model. Tree Physiol 21:889–897.

Pretzsch H (2009) From primary production to growth and harvestable yield and vice versa. Forest dynamics, growth and yield. Springer, Berlin, Heidelberg 41–99.

Reich PB, Sendall KM, Stefanski A, Wei X, Rich RL, Montgomery RA (2016) Boreal and temperate trees show strong acclimation of respiration to warming. Nature 531:633–636.

Rodríguez-Calcerrada J, Martin-StPaul NK, Lempereur M, Ourcival J-M, del Rey MdC, Joffre R, Rambal S (2014) Stem CO2 efflux and its contribution to ecosystem CO2 efflux decrease with drought in a Mediterranean forest stand. Agric For Meteorol 195:61–72.

Rossi S, Deslauriers A, Anfodillo T (2006a) Assessment of cambial activity and xylogenesis by microsampling tree species: an example at the Alpine timberline. IAWA J 27:383–394.

Rossi S, Deslauriers A, Anfodillo T, Morin H, Saracino A, Motta R, Borghetti M (2006b) Conifers in cold environments synchronize maximum growth rate of tree-ring formation with day length. New Phytol 170:301–310.

Roux XL, Lacointe A, Escobar-Gutiérrez A, Dizès SL (2001) Carbon-based models of individual tree growth: a critical appraisal. Ann For Sci 58:469–506.

Ryan MG (1990) Growth and maintenance respiration in stems of Pinus contorta and Picea engelmannii. Can J For Res 20:48–57.

Ryan MG, Cavaleri MA, Almeida AC, Penchel R, Senock RS, Luiz Stape J (2009) Wood CO2 efflux and foliar respiration for Eucalyptus in Hawaii and Brazil. Tree Physiol 29:1213–1222.

Ryan MG, Hubbard RM, Clark DA, Sanford RL (1994) Woody-tissue respiration for Simarouba amara and Minquartia guianensis, two tropical wet forest trees with different growth habits. Oecologia 100: 213–220.

Ryan MG, Gower ST, Hubbard RM, Waring RH, Gholz HL, Cropper WP, Running SW (1995) Woody tissue maintenance respiration of four conifers in contrasting climates. Oecologia 101:133–140.

Ryan MG, Lavigne MB, Gower ST (1997) Annual carbon cost of autotrophic respiration in boreal forest ecosystems in relation to species and climate. J Geophys Res 102:28871–28883.

Salomón RL, Valbuena-Carabaña M, Gil L, McGuire MA, Teskey RO, Aubrey DP, González-Doncel I, Rodríguez-Calcerrada J (2016) Temporal and spatial patterns of internal and external stem CO2 fluxes in a sub-Mediterranean oak. Tree Physiol 36:1409–1421.

Saveyn A, Steppe K, McGuire M, Lemeur R, Teskey R (2008) Stem respiration and carbon dioxide efflux of young Populus deltoides trees in relation to temperature and xylem carbon dioxide concentration. Oecologia 154:637–649.

Sevanto S, Vesala T, Perämäki M, Nikinmaa E (2003) Sugar transport together with environmental conditions controls time lags between xylem and stem diameter changes. Plant Cell Environ 26: 1257–1265.

Sevanto S, Hölttä T, Markkanen T, Perämäki M, Nikinmaa E, Vesala T (2005) Relationships between diurnal xylem diameter variation and environmental factors in Scots pine. Boreal Environ Res 10:447–458.

Sevanto S, Hölttä T, Holbrook NM (2011) Effects of the hydraulic coupling between xylem and phloem on diurnal phloem diameter variation. Plant Cell Environ 34:690–703.

Sperry JS, Sullivan JE (1992) Xylem embolism in response to freeze-thaw cycles and water stress in ring-porous, diffuse-porous, and conifer species. Plant Physiol 100:605–613.

Sprugel DG, Benecke U (1991) Measuring woody-tissue respiration and photosynthesis. In: Lassoie JP, Hinckley TM (eds) Techniques and Approaches in Forest Tree Ecophysiology. CRC Press, Boca Raton, FL, pp 329–355.

Stockfors J, Linder S (1998) Effect of nitrogen on the seasonal course of growth and maintenance respiration in stems of Norway spruce trees. Tree Physiol 18:155–166.

Teskey R, McGuire M (2002) Carbon dioxide transport inxylem causes errors in estimation of rates of respiration in stemsand branches of trees. Plant Cell Environ 25:1571–1577.

Teskey RO, Saveyn A, Steppe K, McGuire MA (2008) Origin, fate and significance of CO2 in tree stems. New Phytol 177:17–32.

Thornley J (1970) Respiration, growth and maintenance in plants. Nature 227:304–305.

Torrence C, Compo GP (1998) A practical guide to wavelet analysis. Bull Am Meteorol Soc 79:61–78.

Trumbore SE, Angert A, Kunert N, Muhr J, Chambers JQ (2013) What's the flux? Unraveling how CO2 fluxes from trees reflect underlying physiological processes. New Phytol 197:353–355.

Ubierna N, Kumar AS, Cernusak LA, Pangle RE, Gag PJ, Marshall JD (2009) Storage and transpiration have negligible effects on 13C of stem CO2 efflux in large conifer trees. Tree Physiol 29: 1563–1574.

Vargas R, Baldocchi DD, Bahn M, Hanson PJ, Hosman KP, Kulmala L, Pumpanen J, Yang B (2011) On the multi-temporal correlation between photosynthesis and soil CO2 efflux: reconciling lags and observations. New Phytol 191:1006–1017.

Vesala T, Suni T, Rannik Ü et al. (2005) Effect of thinning on surface fluxes in a boreal forest. Global Biogeochem Cycles 19:1–11.

Vose JM, Ryan MG (2002) Seasonal respiration of foliage, fine roots, and woody tissues in relation to growth, tissue N, and photosynthesis. Glob Chang Biol 8:182–193.

Xiao C-W, Yuste JC, Janssens I, Roskams P, Nachtergale L, Carrara A, Sanchez B, Ceulemans R (2003) Above- and belowground biomass and net primary production in a 73-year-old Scots pine forest. Tree Physiol 23:505–516.

Zha T, Kellomäki S, Wang K-Y, Ryyppö A, Niinistö S (2004) Seasonal and annual stem respiration of Scots pine trees under boreal conditions. Ann Bot 94:889–896.

Zumer M (1969) Annual ring formation in Norway spruce in mountain forest. [Norweg.; Eng. summ.]. Medd Norske Skogsforsoksv 27:161–184.

Zweifel R (2016) Radial stem variations – a source of tree physiological information not fully exploited yet. Plant Cell Environ 39:231–232.